Utilization of Waste Natural Fiber Mixed with Polylactic Acid (PLA) Bicomponent Fiber: Incorporating Kapok and Cattail Fiber for Nonwoven Medical Textile Applications

Tanyalak Srisuk , Khanittha Charoenlarp , Piyaporn Kampeerapappun *

Posted Date: 12 December 2023

doi: 10.20944/preprints202312.0874.v1

Keywords: cattail fiber; kapok fiber; polylactic acid; nonwoven; hot-press; bicomponent fiber

Article

Utilization of Waste Natural Fiber Mixed with Polylactic Acid (PLA) Bicomponent Fiber: Incorporating Kapok and Cattail Fiber for Nonwoven Medical Textile Applications

Tanyalak Srisuk, Khanittha Charoenlarp and Piyaporn Kampeerapappun *

Faculty of Textile Industries, Rajamangala University of Technology Krungthep, Bangkok, Thailand
* Correspondence: piyaporn.k@mail.rmutk.ac.th

Abstract: Disposable surgical gowns are usually made from petroleum-based synthetic fibers that do not naturally decompose, impacting the environment. A promising approach to diminish the environmental impact of disposable gowns involves utilizing natural fibers and/or bio-based synthetic fibers. In this study, composite web from polylactic bicomponent fiber and natural fibers, cattail and kapok fiber, were prepared by hot-press method. Only the sheath region of the PLA bicomponent fiber melts, acting as an adhesive that enhanced the strength and reduced the thickness of the composite web compared to its state before hot-pressing. Mechanical and physical properties of composite webs were evaluated. Composite webs created from kapok fiber displayed a creamy yellowish-white color, while those made from cattail fiber showed a yellowish-brown color. Composite webs exhibit hydrophobic properties when adding the natural fiber. The maximum natural fiber content, at a ratio of 30, can be incorporated into composite webs while preserving mechanical properties and proper water vapor permeability. This nonwoven material presents an alternative with the potential to replace petroleum-based surgical gowns.

Keywords: cattail fiber; kapok fiber; polylactic acid; nonwoven; hot-press; bicomponent fiber

1. Introduction

The COVID-19 pandemic has led to the global consumption of billions of face masks, contributing to significant plastic waste [1,2]. Despite polypropylene (PP) being a cost-effective primary material in personal protective equipment, concerns have arisen regarding its reliance on diminishing petroleum sources and its significant environmental impact [3]. Consequently, there has been a noticeable drive in recent years to substitute various petroleum-based products with natural, sustainable, and eco-friendly alternatives [4,5]. This pursuit has prompted an exploration of sustainable materials across industries, particularly a keen interest in natural fibers for composite materials. This interest is mainly because of its renewability, low cost, low density, and low abrasiveness of the natural materials in the polymer industry [6,7].

Numerous research studies on natural fibers for nonwoven materials have been published. For instance, milkweed has demonstrated potential for blending with bicomponent fibers and hot-pressing to create a composite web, offering a potentially environmentally friendly alternative to current petroleum-based disposable surgical gown [8]. Fages et al. [9] combined flax with polypropylene fibers using a wet-laid process, preparing them for subsequent hot-press molding. The combination of wet-laid techniques with hot-press molding processes enables the utilization of high natural fiber content in composite webs while maintaining acceptable properties. Ghali et al. [10] utilized the needle-punching method to blend alfa fibers with cotton, polyester, Tencel®, and wool. Their observations indicated that the air permeability of nonwoven blends generally increased with the higher ratio of alfa fiber, except in the wool blend. Additionally, Möhl et al. [11] employed

 doi:10.20944/preprints202312.0874.v1

cellulosic fibers sourced from textile waste along with polymers derived from renewable raw materials, proposing a potential approach for upcycling textile waste.

Among natural fibers, cattail and kapok fibers have gained recent attention owing to their widespread availability and notable features, including low density and hydrophobic-oleophilic properties [12–14]. Cattail, known as water candle, is an aquatic plant found in temperate and tropical regions across both hemispheres, thriving in various aquatic environments such as lakes, rivers, swamps, ponds, and ditches. When reaching maturity, cattail grass exhibits a unique behavior, bursting and releasing a substantial amount of cattail fibers, posing potential risks of pollution or fires [12]. Similarly, kapok fiber, known for its thin cell wall and large lumen, has traditionally found use as stuffing material in items like pillows and life jackets [14,15]. In addition, the development of environmentally friendly bio-based materials has also been accelerated by the pursuit of sustainable practices; one such material is polylactic acid (PLA), which has been used to have a significant impact. PLA is a biodegradable and bioactive polyester derived from renewable resources such as corn, potato, sugarcane or other carbohydrate sources [16,17]. It is commonly used in various applications, including packaging [18], biomedical devices [19], 3D printing [19], and textiles [19–21], due to its eco-friendly nature and biodegradability [22,23].

In this research, the focus was on developing a medical nonwoven material with specific properties such as antibacterial qualities, water repellency, light weight, and proper air permeability. To achieve this, both milkweed and kapok fibers was utilized, known for their low density and hydrophobic properties. Blending them with PLA bicomponent fiber, a biodegradable polymer, was the approach taken to create the desired nonwoven material with the targeted properties for medical applications.

2. Materials and Methods

2.1. Materials

A sheath-core polylactic acid bicomponent fiber with a length of 38 mm and 2.24 dtex was purchased from Tianjin Glory Tang Textile Co., Ltd. (Tianjin, China). Kapok and cattail fibers were collected locally in Bangkok, Thailand. Seeds and other impurities in the kapok and cattail fibers were manually removed. The fibers were used in their raw state in the experiment without any chemical cleaning or pre-treatment processes.

2.2. Preparation of natural fiber/polylactic acid bicomponent fiber composite webs

The natural fiber/polylactic acid bicomponent fiber composites were produced with blend ratios ranging from 0/100 to 30/70 by weight using carding and hot-press techniques. A Y275A hand-operated drum-carding machine (SDL Atlas Limited, Hong Kong) was used to card the hand-blended fiber. This procedure was repeated 3 times to ensure that the materials were thoroughly mixed and to ensure that the fibers were distributed uniformly. After the carding process, the webs are placed into a circular mold with an 11 cm diameter on a heat press machine and then manually hot-pressed at 135°C for 1 minute to achieve a target weight of 100 g/m^2.

2.3. Characterizations

SEM images of the fibers and composite webs were recorded using Jeol JSM-6400 scanning electron microscope (Jeol Ltd., Japan). A 204 F1 Phoenix model differential scanning calorimetry (DSC) instrument (Netzsch-Gerätebau GmbH, Germany) was used to determine specific heat capacity of both natural and bicomponent fibers. The samples in an aluminum pan were heated from room temperature to 450°C at a rate of 10°C/min under a nitrogen atmosphere. The thickness values of composite webs at various ratios were measured using a 547-401A Mitutoyo digital thickness gauge (Mitutoyo, Japan).

2.4. Properties

 doi:10.20944/preprints202312.0874.v1

2.4.1. Color measurement

The CIE L*a*b* values and whiteness of composite webs were measured using the Datacolor Check II spectrophotometer (Datacolor, USA) under D65 illuminant and a 10-degree observer angle.

2.4.2. Contact angle measurements

The tests were performed according to BS EN 828:2013 standard using DM-CE1 contact angle meters (Kyowa Interface Science Co. Ltd., Japan). Briefly, each droplet of deionized water, precisely 2 μL in volume, was carefully deposited onto the sample surface and measured after a 10 second interval. All measurements were conducted at a temperature of 21 ± 1 °C and a relative humidity of 65 ± 2%. Each sample underwent testing at a minimum of three different locations.

2.4.3. Antibacterial Activity

The PLA, cattail fiber, and kapok fiber were evaluated against the Gram-negative bacteria K. pneumoniae and Gram-positive bacteria S. aureus following the ASTM E2149 standard. Dynamic conditions involved 100 rpm at 37 C for 18 hours. The experiment was conducted in triplicate. After incubation, colonies were counted to determine the bacterial count. The percentage of bacterial reduction (R, %) was calculated in accordance with Equation 1:

$$R = \frac{C_0 - C}{C_0} \times 100 \quad (1)$$

where R is the percentage of reduction bacteria viability

C_0 is the number of bacteria colonies at contact time = 0 h

C is the number of bacteria colonies after contact time

2.4.4. Mechanical test

The tensile properties were evaluated using a M350-5AT Testometric universal testing machine (Testometric Company Ltd., UK) with a crosshead speed of 5 mm/min and a load cell capacity of 50 kN. Rectangular specimens, sized at 10 × 60 mm, were cut using compression molded plates for the tests with a gauge length of 40 mm. A minimum of five samples were tested for each group of samples.

2.4.5. Water vapor permeability analysis

The water vapor permeability was assessed using the evaporative dish method, in accordance with the BS 7209 standard. The test involved securing the test specimen over the open mouth of a dish filled with water and measuring the initial weight of the cup. After a 6-hour period, the weight was recorded again to assess any changes. Water vapor permeability (WVP) was calculated (Equation 2).

$$\text{Water vapor permeability (WVP)} = \frac{24.M}{A.T} \quad (2)$$

where M is the loss in mass (g) of water vapor through the fabric specimen

A is the internal area of the dish (m^2)

T is the time between weighing (h)

3. Results and Discussion

3.1. Characterization of fibers

Waste natural fibers, including cattail and kapok fibers, have distinct characteristics. Cattail fibers feature a multi-cavity structure, bamboo-shaped and average length of 10 mm, while kapok fibers have an average length of 20 mm and a hollow lumen structure (Figure 1a,b). The sheath-core PLA bicomponent fiber, depicted in Figure 1c, has a diameter of approximately 20 μm, with the sheath measuring around 2 μm in thickness.

Preprints (www.preprints.org) | NOT PEER-REVIEWED | Posted: 12 December 2023 doi:10.20944/preprints202312.0874.v1

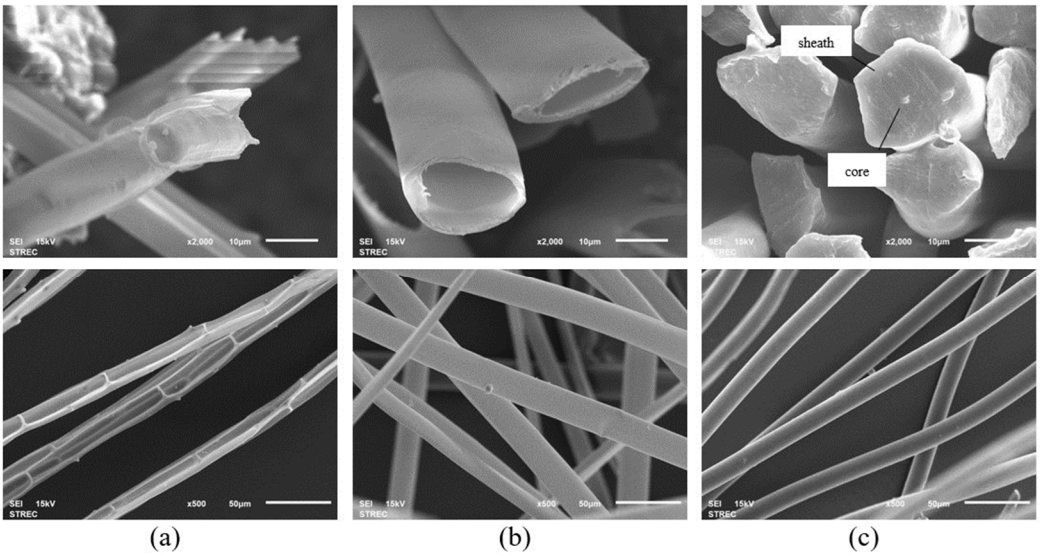

Figure 1. Cross-sectional and longitudinal SEM images of (a) cattail fiber (b) kapok fiber (c) PLA bicomponent fiber.

DSC thermograms for both kapok fiber and cattail fiber exhibited similarity (Figure 2a,b). The results from the thermograms suggest that the initial weight loss occurred below 100°C, attributed to the presence of water in the fiber [24]. The first exothermic peak appeared around 280-310°C, indicating the degradation of cellulose. The second exothermic peak at 330-370°C is likely associated with the oxidation of the char [25,26]. The used PLA bicomponent fiber exhibits two melting peaks at 131.3°C and 174.3°C. It is worth noting that the degradation temperature of PLA falls within the range of 330-380°C (Figure 2c). These findings are similar to those of Kervran et al. 2022 [27], where PLA degrades in one step around 350°C.

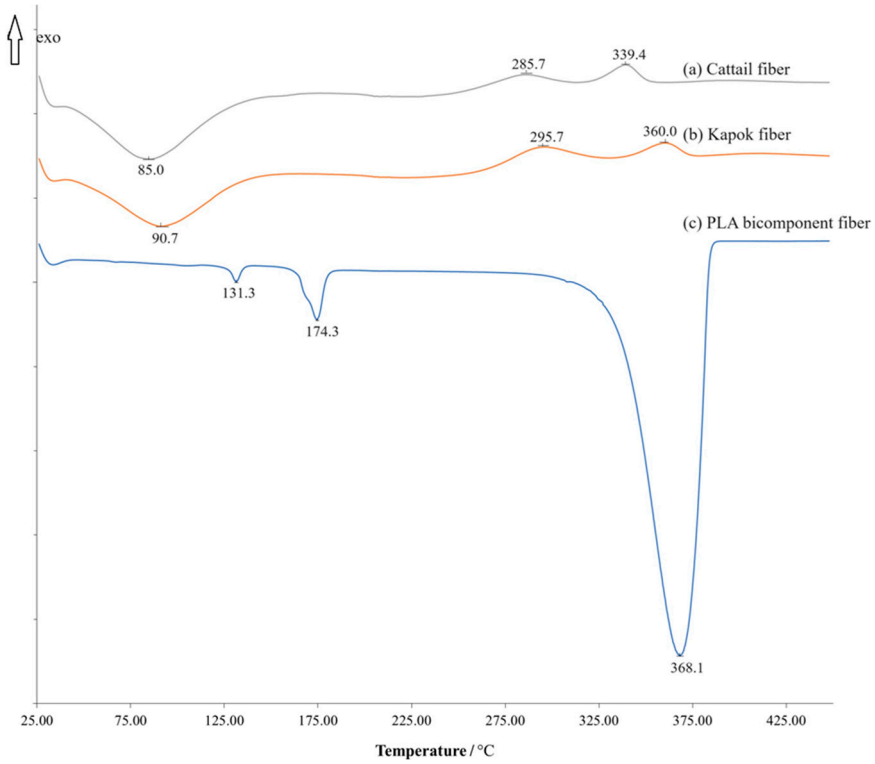

Figure 2. DSC thermogram (a) cattail fiber (b) kapok fiber (c) PLA bicomponent fiber.

 doi:10.20944/preprints202312.0874.v1

From the literature review, it is indicated that both cattail and kapok fibers exhibit natural antibacterial activity due to their high lignin content [28–30]. Cattail fiber contains an approximate lignin content of 16.5% [30], while kapok fiber exhibits a lignin content ranging from 13% to 22% [29]. In this study, the antibacterial efficacy of these fibers was evaluated according to the ASTM E2149 standard against *S. aureus* and *K. pneumoniae*. The results are presented in the Table 1.

Table 1. Antibacterial activity of fibers against *S. aureus* and *K. pneumonia* bacteria after contact time.

Type of bacteria	Bacterial reduction (%)		
	Cattail fiber	Kapok fiber	PLA bicomponent fiber
S. aureus	7.78	16.73	1.41
K. pneumoniae	-8.25	-6.98	-7.51

It appears that all the tested fibers did not exhibit antibacterial activity against *K. pneumoniae*. However, they showed a limited antibacterial effect against *S. aureus*. Kapok fiber demonstrated the most substantial reduction in bacterial activity when compared to both cattail and PLA bicomponent fibers. The antibacterial properties of the composite web samples were not tested since all tested fibers displayed minimal antibacterial activity.

3.2. Characterization of composite webs

After the carding process, the obtained webs exhibited a fluffy texture and had low mechanical properties, primarily attributed to the absence of chemical or physical bonding among the fibers. To improve adhesion, chemical or thermal binders are commonly used. In this study, the carded webs were hot-pressed at 135°C, a temperature higher than the melting point of the sheath but lower than the melting point of the core fibers. The composite webs underwent testing for thickness, color, and mechanical properties.

3.2.1. Thickness

The thickness values of the composite webs are presented in Table 2.

Table 2. Thickness values of the composite webs.

PLA: natural fiber ratio	Thickness (mm)	
	PLA: cattail fiber	PLA: kapok fiber
100: 0	0.2594 ± 0.0294	
90: 10	0.3436 ± 0.0126	0.3798 ± 0.0168
80: 20	0.3606 ± 0.0189	0.3812 ± 0.0168
70: 30	0.4080 ± 0.0211	0.4268 ± 0.0251
60: 40	0.4686 ± 0.0148	0.5023 ± 0.0265
50: 50	0.5288 ± 0.0170	0.5648 ± 0.0449
40: 60	0.5468 ± 0.0304	0.7020 ± 0.1066
30: 70	0.6286 ± 0.0938	0.8252 ± 0.1171

As shown in Table 2, the increase in both cattail and kapok fiber content led to an augmentation in the thickness of the composite webs. This outcome can be attributed to the notably low density of both cattail and kapok fibers. In nonwoven materials determined by weight (g/m^2), the incorporation of these fibers with the same weight resulted in thicker nonwoven structures due to their low density. These observations are consistent with a previous study involving poly(lactic acid)/poly(butylene succinate) (PLA/PBS) fiber and milkweed fiber. In that study, it was noted that increasing the ratio of

Preprints (www.preprints.org) | NOT PEER-REVIEWED | Posted: 12 December 2023 doi:10.20944/preprints202312.0874.v1

milkweed fiber resulted in enhanced thickness in the composite material [8]. Additionally, when comparing PLA: kapok fiber composite webs to PLA: cattail fiber composite webs at the same ratio, the composite webs from PLA: kapok fiber exhibited greater thickness. Kapok fiber holds the distinction of being the lightest natural fiber globally. Studies by Mwaikambo (2006) [31] and Sekar et al. [32] report the bulk density of kapok at 0.38 g/cm^3, whereas cattail fiber's density is recorded at 0.62 g/cm^3 [33].

3.2.2. Color measurement

The images of composite webs were depicted in Figure 3, while measurements for whiteness index and CIE L*a*b* values of these composite webs were recorded and presented in Table 3.

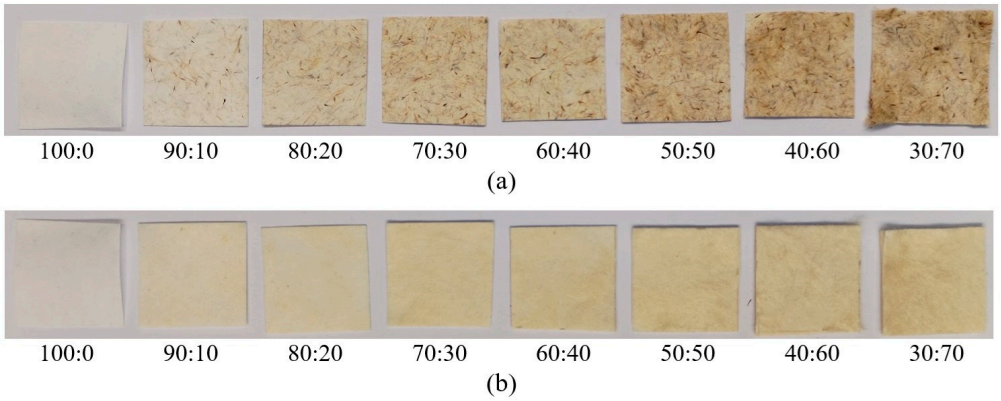

Figure 3. Appearance of the PLA composite with natural fiber at different ratios (a) PLA: cattail fiber (b) PLA: kapok fiber.

Table 3. Whiteness and CIE L*a*b* values of composite webs.

PLA: natural fiber	PLA: cattail fiber				PLA: kapok fiber			
ratio	WI [1]	L*	a*	b*	WI	L*	a*	b*
100: 0	86.49	94.71	-0.20	0.08	86.49	94.71	-0.20	0.08
90: 10	44.98	87.09	1.71	4.89	48.54	90.12	-0.18	6.31
80: 20	9.86	85.35	1.58	6.86	34.28	88.87	1.09	8.13
70: 30	30.84	84.00	2.36	7.38	21.77	87.69	1.49	10.07
60: 40	-6.86	76.90	2.78	9.74	16.85	86.85	1.81	10.60
50: 50	-21.85	74.04	3.84	11.05	7.02	85.68	2.23	11.94
40: 60	-61.94	71.31	5.15	16.08	-3.17	84.38	2.46	13.25
30: 70	-57.00	70.48	5.29	16.52	-4.38	83.20	2.29	13.47

[1] WI is whiteness index.

The whiteness index tends to decrease with an increase in the content of natural fibers added to the PLA fiber. Additionally, the whiteness index of composite webs made from cattail fiber is lower than that of kapok fiber at the same ratio. (Table 3). The color differentiation between kapok and cattail fibers is commonly observed, with kapok fibers typically appearing creamy -yellowish white, while cattail fibers tend to have a light yellowish-brown shade.

The CIE L*a*b* system comprises three values: L* (white-black), a* (red-green), and b* (yellow-blue). Higher L* values indicate a whiter appearance, while higher a* and b* values suggest more reddish and yellowish tones, respectively. With an increased natural fiber content in both cattail and kapok fibers, there is a decrease in the L* value, indicating a darker hue, and an increase in the b* value, suggesting a more yellowish coloration. Furthermore, the a* values of composite webs show a

Preprints (www.preprints.org) | NOT PEER-REVIEWED | Posted: 12 December 2023 doi:10.20944/preprints202312.0874.v1

slight increase with higher natural fiber content, indicating a tendency towards a more reddish hue in these webs.

3.2.3. Morphology of composite webs

During the hot-press process at a temperature of 135°C, the bicomponent fibers experience partial melting, which subsequently leads to the adhesion of natural fibers and bicomponent fibers together, as depicted in the Figures 4 and 5. At this specific hot-press temperature, the core of the PLA bicomponent remains solid, preserving the fibrous structure instead of forming a film-like structure. Meanwhile, the molten PLA sheath possesses adhesive properties, enabling it to adhere to neighboring fibers. As the proportion of natural fiber increases, the presence of PLA bicomponent fibers diminishes. When the PLA ratio exceeds 50%, it becomes challenging for the PLA to retain both natural fibers. Consequently, the composite webs might exhibit the fluffiness characteristic of natural fibers at this stage (Figure 3).

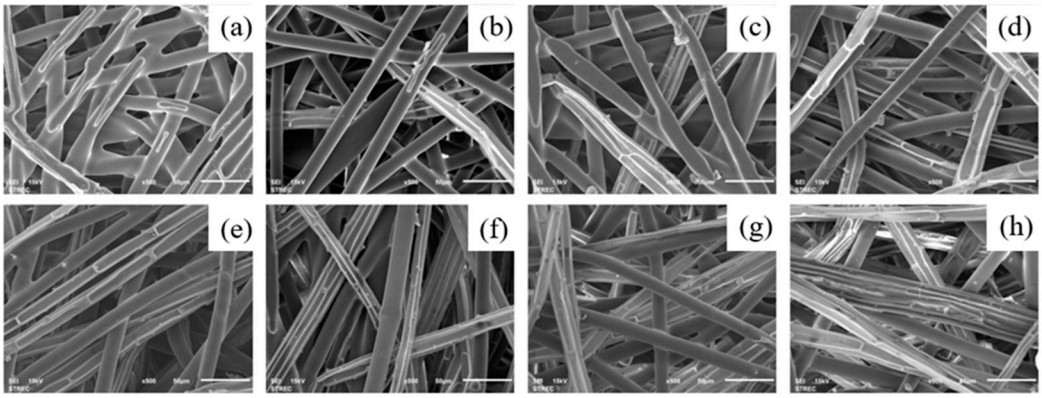

Figure 4. SEM images of PLA: cattail fibers composite webs at ×500 magnification (a) 100:0 (b) 90:10 (c) 80:20 (d) 70:30 (e) 60:40 (f) 50:50 (g) 40:60 (h) 30:70.

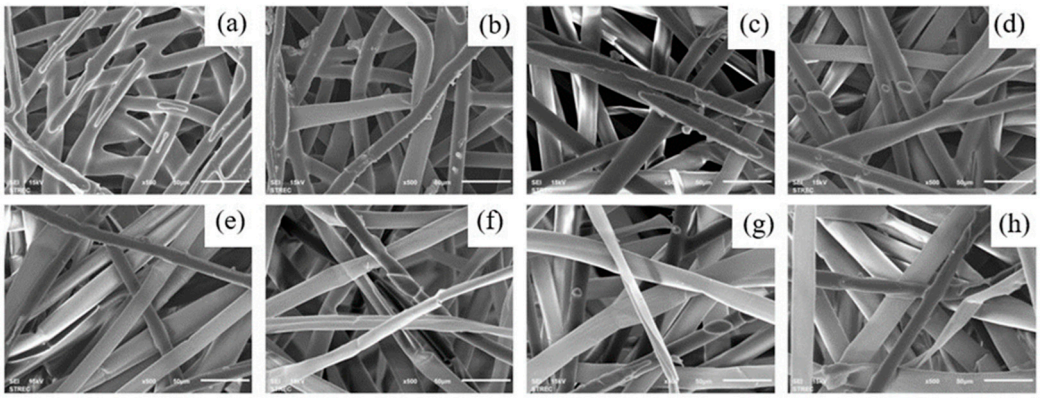

Figure 5. SEM images of PLA: kapok fibers composite webs at 500 magnification (a) 100:0 (b) 90:10 (c) 80:20 (d) 70:30 (e) 60:40 (f) 50:50 (g) 40:60 (h) 30:70.

3.2.4. Mechanical test

The mechanical properties of the composite webs were tested and the data are presented in Table 4. Additionally, the stress-strain curves of these composite webs are displayed in Figure 6.

Preprints (www.preprints.org) | NOT PEER-REVIEWED | Posted: 12 December 2023 doi:10.20944/preprints202312.0874.v1

Table 4. Mechanical properties of composite webs.

Sample	PLA: natural fiber	Ultimate load (N)	Young's modulus (MPa)	Elongation at break (%)	Yield strength (MPa)	Yield strain (%)
PLA	100: 0	47.08 ± 2.01	551.76 ± 10.75	8.17 ± 0.64	10.62 ± 0.90	5.99 ± 0.14
PLA: cattail fiber	90:10	45.48 ± 2.85	570.29 ± 12.25	7.90 ± 0.46	10.85 ± 0.65	5.84 ± 0.07
	80:20	33.95 ± 0.97	523.71 ± 5.60	4.07 ± 0.83	8.71 ± 0.20	4.79 ± 0.50
	70:30	21.18 ± 2.53	309.72 ± 12.11	4.33 ± 1.47	4.44 ± 0.80	3.91 ± 0.45
	60:40	15.10 ± 0.88	279.23 ± 13.57	3.26 ± 0.96	3.70 ± 0.43	2.33 ± 0.97
	50:50	7.23 ± 0.68	153.95 ± 13.45	3.68 ± 0.89	1.84 ± 0.08	2.75 ± 0.40
	40:60	7.01 ± 0.87	115.84 ± 8.14	3.36 ± 0.78	1.63 ± 0.22	2.68 ± 0.71
	30:70	6.02 ± 0.79	117.28 ± 10.44	3.64 ± 0.60	1.41 ± 0.22	2.11 ± 0.52
PLA: kapok fiber	90:10	42.19 ± 3.91	408.35 ± 23.61	6.79 ± 0.24	9.43 ± 1.22	4.37 ± 0.62
	80:20	39.88 ± 3.08	451.37 ± 35.69	6.42 ± 0.31	10.83 ± 0.57	4.76 ± 0.65
	70:30	22.46 ± 1.58	295.28 ± 48.84	6.55 ± 0.81	7.10 ± 1.52	4.51 ± 0.84
	60:40	18.13 ± 2.16	224.79 ± 35.02	3.96 ± 1.46	3.82 ± 0.22	2.67 ± 0.97
	50:50	15.81 ± 0.19	170.42 ± 14.75	4.45 ± 0.65	3.85 ± 0.93	2.56 ± 0.72
	40:60	8.44 ± 0.12	129.35 ± 1.83	3.67 ± 0.48	1.85 ± 0.29	2.16 ± 0.74
	30:70	1.59 ± 0.03	21.73 ± 6.72	9.77 ± 0.01	0.25 ± 0.01	1.87 ± 0.34

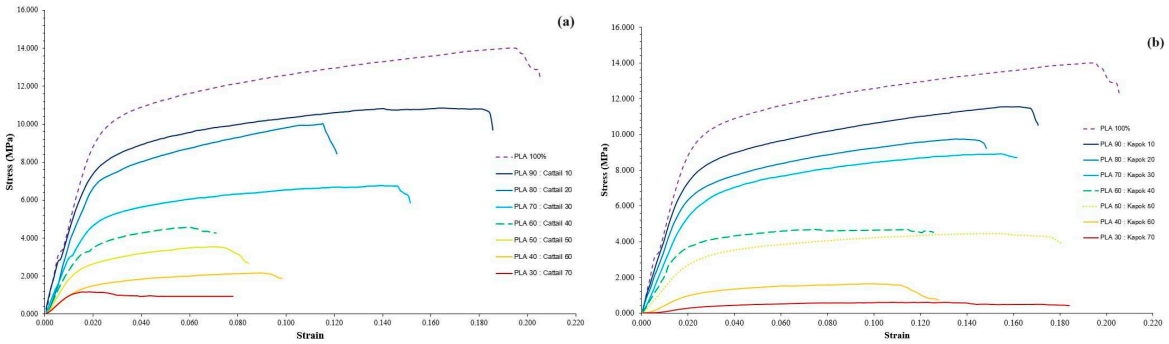

Figure 6. Stress-strain curves of composite webs comprising PLA bicomponent fiber mixed with (a) cattail fiber and (b) kapok fiber.

Higher natural fiber content in the PLA bicomponent fiber composite webs results in reduced ultimate load, Young's modulus, yield strength, and yield strain. At the same natural fiber level, composite webs with kapok fiber generally exhibit better mechanical properties than those mixed with cattail fiber, except in the case of PLA: cattail fiber at a 30:70 ratio. This could be attributed to the longer fiber length of kapok fiber, leading to improved interfacial bonding properties. As noted by Du et al. [34], long glass fiber composite materials tend to exhibit superior mechanical properties compared to short glass fiber composites. At a 30:70 ratio of PLA: kapok fiber, the lower density of kapok fibers compared to cattail fibers results in a higher fiber content within the composite webs. Consequently, the PLA bicomponent fibers may struggle to effectively bind all the fibers, leading to significantly reduced mechanical properties

In our study, only the sheath of the bicomponent fibers melts and acts as an adhesive to bind the natural fibers. However, a high ratio of natural fibers coupled with a low density results in the adhesive being unable to secure all natural fibers, leading to reduced mechanical properties (Table 4). Composite webs containing over 40% natural fibers exhibit diminished mechanical properties, a trend consistent with the findings of Mula et al.'s study [8]. This finding aligns with the observation

Preprints (www.preprints.org) | NOT PEER-REVIEWED | Posted: 12 December 2023 doi:10.20944/preprints202312.0874.v1

that at higher ratios of natural fibers in these composite webs, a fluffy appearance emerges, attributed to an increased content of fibers within the web structure (Figure 3). In addition, according to the EN 13795-2: 2019 standard, the tensile strength requirement for protective clothing in the dry state is equal to or greater than 20 N. In this context, when the natural fiber ratio equals or falls below 30, the material demonstrates an ultimate load higher than this specified standard.

3.2.5. Water contact angle measurement

Surgical gowns should repel blood, body fluids, and other contaminants to ensure that these substances do not penetrate the gown. This characteristic helps maintain the sterility of the gown and prevents the transmission of infectious agents between the medical professional and the patient during surgical procedures. The contact angle of a water drop on the composite webs is illustrated in Figure 7.

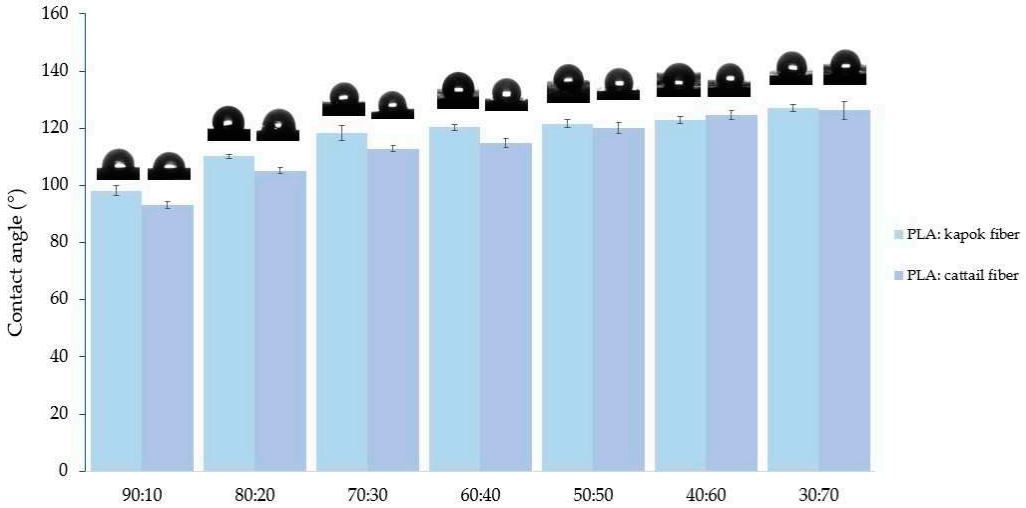

Figure 7. Water contact angle of composite webs.

Contact angle values range between 0° and 180°. A contact angle of 0° corresponds to complete wetting, while an angle of 180° indicates non-wetting. A material is considered superhydrophobic if the contact angle is greater than 150°.

The PLA bicomponent web cannot detect water contact angles as it absorbs water immediately. However, the water contact angle increased with a higher natural fiber content in composite webs, as depicted in the Figure 7. Ranging from 98° to 127°, the water contact angle of composite webs highlights their hydrophobic nature. This phenomenon is attributed to the surface wax present in both cattail and kapok fibers, contributing to their hydrophobic and oleophilic properties [35–37]. Studies by Abdullah et al. [38] reported a wax content of approximately 3% in kapok fiber, while Draman et al. [39] noted a higher content of 5.51%. Based on Soxhlet extraction, Wu et al. [40] reported that wax on the surface of cattail fibers accounted for 11.5%. When comparing both natural fibers at the same ratio, cattail fiber in composite webs exhibits a slightly lower water contact angle than kapok fiber. This difference may be attributed to the lower density of kapok fiber. Consequently, at an equivalent weight, kapok fiber possesses a higher volume of fibers compared to cattail fiber. The results indicate that blending natural fibers with PLA bicomponent fibers aids in providing better protection against blood and body fluids compared to using only PLA bicomponent fiber webs.

3.2.6. Water vapor permeability analysis

Breathability is the ability of textile allowing water vapor from the body through it while preventing liquid from entering from the outside [41]. This characteristic plays a crucial role in determining comfort, often assessed through the measurement of moisture vapor transmission rate.

Preprints (www.preprints.org) | NOT PEER-REVIEWED | Posted: 12 December 2023 doi:10.20944/preprints202312.0874.v1

The water vapor permeability of the composite webs was tested, and the results are presented in Figure 8.

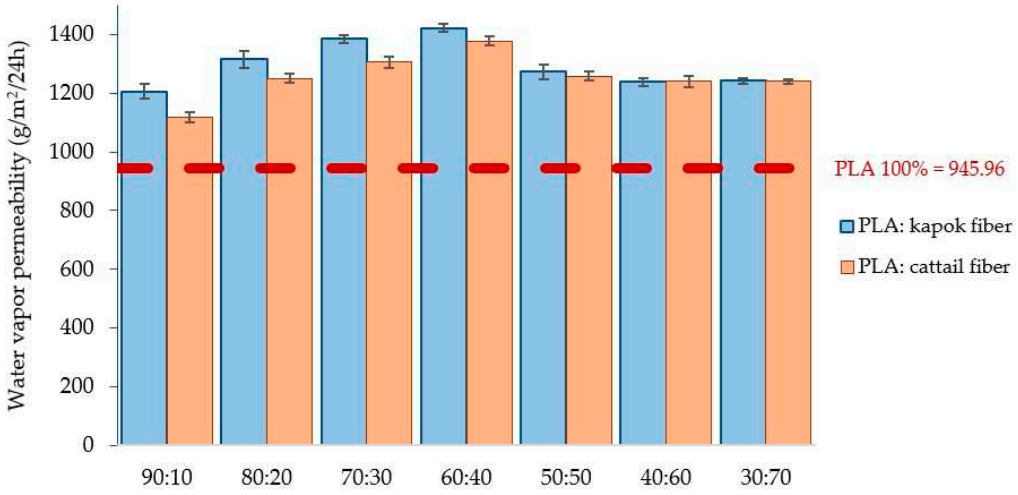

Figure 8. Water vapor permeability values of the composite webs.

Incorporating natural fibers into the composite webs enhances their water vapor permeability compared to 100% PLA bicomponent webs. Interestingly, composite webs made from cattail fibers exhibit lower water vapor permeability than those crafted from kapok fibers at identical ratios. Several factors influence water vapor permeability, including sample thickness; thicker samples increase the distance and time needed for water vapor to travel, resulting in reduced permeability. Despite composite webs from kapok fibers being slightly thicker than those from cattail fibers at the same ratio, the significant lumen present in kapok fibers contributes to their higher water vapor permeability [42].

The information from Kannekens [43] and Behera and Arora [41] classifies the water vapor permeability rates of breathable surgical gowns at 20°C into different categories: moderate (360 g/m²/24h), high (1392 g/m²/24h), and very high (2400 g/m²/24h). All composite webs show moderate rates, ranging from 945-1384 g/m²/24h, except for the PLA: kapok fiber at 60:40, which exhibits a high water vapor permeability rate of 1421 g/m²/24h. There might be a need in future work to reduce the thickness of composite webs to enhance water vapor permeability.

4. Conclusions

Composite webs composed of polylactic acid bicomponent fibers combined with both waste natural fibers were successfully prepared. Cattail fiber was bamboo-shaped structure, while kapok fiber exhibited a hollow tube structure. SEM images demonstrated that the composite web maintained a fibrous structure rather than forming a film-like structure. Evaluation of mechanical and physical properties was conducted, revealing distinctive color characteristics—creamy yellowish-white for kapok fiber-based webs and yellowish-brown for cattail fiber-based webs. While the incorporation of natural fibers might reduce the mechanical properties of the composite web, it has a beneficial impact on enhancing water vapor permeability and achieving a higher water contact angle, thereby protecting against water droplets penetrating the fabric.

Author Contributions: Conceptualization, P.K.; methodology, P.K.; investigation, P.K. and T.S.; resources, P.K. and K.C.; writing—original draft preparation, P.K. and T.S.; writing—review and editing, P.K..; visualization, P.K. and T.S.; supervision, P.K. All authors have read and agreed to the published version of the manuscript.

Data Availability Statement: The data presented in this study are available on request from the corresponding author.

Conflicts of Interest: The authors declare no conflict of interest.

References

1. Benson, N.U.; Bassey, D.E.; Palanisami, T. COVID Pollution: Impact of COVID-19 Pandemic on Global Plastic Waste Footprint. *Heliyon*. **2021**, 7(2), e06343. doi: 10.1016/j.heliyon.2021.e06343
2. Wang, L.; Li, S.; Ahmad, I.M.; Zhang, G.; Sun, Y.; Wang, Y.; Sun, C.; Jiang, C.; Cui, P.; Li, D. Global Face Mask Pollution: Threats to the Environment and Wildlife, and Potential Solutions. *Sci Total Environ*. **2023**, 887, 164055. doi: 10.1016/j.scitotenv.2023.164055
3. Cubas, A.L.V.; Moecke, E.H.S.; Provin, A.P.; Dutra, A.R.A.; Machado, M.M.; Gouveia, I.C. The Impacts of Plastic Waste from Personal Protective Equipment Used during the COVID-19 Pandemic. *Polymers.* **2023**, 15(15), 3151. doi: 10.3390/polym15153151
4. Singh, N.; Ogunseitan, O.A.; Wong, M.H.; Tang, Y. Sustainable Materials Alternative to Petrochemical Plastics Pollution: A Review Analysis. *Sustainable Horizons*. **2022**, 2, 100016. doi: 10.1016/j.horiz.2022.100016.
5. Mangal, M.; Rao, C.V.; Banerjee, T. Bioplastic: An Eco-Friendly Alternative to Non-Biodegradable Plastic. *Polym. Int.* **2023**, 72(11), 984-996. doi: 10.1002/pi.6555
6. Jawahar, V.; Gabriel, M.; Santhanam, S.; Selvaraj, S.K. Sustainable Waste Cotton and Pigeon Pea Stalk Fibers Composite Materials for Acoustics and Thermal Properties. *J. Eng. Fibers Fabr.* **2023**, 18. doi:10.1177/15589250231189814
7. Maiti, S.; Islam, M.R.; Uddin, M.A.; Afroj, S.; Eichhorn, S.J. Karim, N. Sustainable Fiber-Reinforced Composites: A Review. *Adv. Sustain. Syst.* **2022**, 6(11), 2200258. doi: 10.1002/adsu.202200258
8. Mula, M.; Tekbaş, R.N.; Cengiz, F.; Yüksek, İ.Ö.; Gürarslan, A. Sustainable Milkweed Fiber Composites for Medical Textile Application. *ACS Sustainable Chem. Eng*. **2023**, 11(34), 12523–12531. doi: 10.1021/acssuschemeng.3c01508
9. Fages, E.; Gironés, S.; Sánchez-Nacher, L.; García-Sanoguera, D.; Balart, R. Use of Wet-Laid Techniques to form Flax-Polypropylene Nonwovens as Base Substrates for Eco-Friendly Composites by Using Hot-Press Molding. *Polym. Compos.* **2012**, 33(2), 253–261. doi: 10.1002/pc.22147
10. Ghali, L.; Halimi, M.T.; Hassen, M.B.; Sakli, F. Effect of Blending Ratio of Fibers on the Properties of Nonwoven Fabrics Based of Alfa Fibers. *AMPC*. **2014**, 4, 116-125. doi: 10.4236/ampc.2014.46014
11. Möhl, C.; Weimer, T.; Caliskan, M.; Baz, S.; Bauder, H.-J.; Gresser, G.T. Development of Natural Fibre-Reinforced Semi-Finished Products with Bio-Based Matrix for Eco-Friendly Composites. *Polymers*. **2022**, 14, 698. doi: 10.3390/polym14040698
12. Cui, F.; Li, H.; Chen, C.; Wang, Z.; Liu, X.; Jiang, G.; Cheng, T.; Bai, R.; Song, L. Cattail Fibers as Source of Cellulose to Prepare a Novel Type of Composite Aerogel Adsorbent for the Removal of Enrofloxacin in Wastewater. *Int. J. Biol. Macromol*. **2021**, 191, 171-181.
13. Zheng, Y.; Wang, J.; Zhu, Y.; Wang, A. Research and Application of Kapok Fiber as an Absorbing Material: A Mini Review. *J. Environ. Sci.* **2015**, 27, 21-32. doi: 10.1016/j.jes.2014.09.026
14. Zerga, A.Y.; Tahir, M. Biobased Kapok Fiber Nano-Structure for Energy and Environment Application: A Critical Review. *Molecules*. **2022**, 27, 8107. doi: 10.3390/molecules27228107
15. Sangalang, R. Kapok Fiber- Structure, Characteristics and Applications: A Review. *Orient. J. Chem*. **2021**, 37(3):513-523. doi: 10.13005/ojc/370301
16. Ilyas, R.A.; Sapuan, S.M.; Harussani, M.M.; Hakimi, M.Y.A.Y.; Haziq, M.Z.M.; Atikah, M.S.N.; Asyraf, M.R.M.; Ishak, M.R.; Razman, M.R.; Nurazzi, N.M.; Norrrahim, M.N.F., Abral, H.; Asrofi, M. Polylactic Acid (PLA) Biocomposite: Processing, Additive Manufacturing and Advanced Applications. *Polymers*. **2021**, 13, 1326. doi: 10.3390/polym13081326
17. Wu, Y.; Gao, X.; Wu, J.; Zhou, T.; Nguyen, T.T.; Wang, Y. Biodegradable Polylactic Acid and Its Composites: Characteristics, Processing, and Sustainable Applications in Sports. *Polymers*. **2023**, 15, 3096. doi: 10.3390/polym15143096
18. Shao, L.; Xi, Y.; Weng, Y. Recent Advances in PLA-Based Antibacterial Food Packaging and Its Applications. *Molecules*. **2022**. 27(18), 5953. doi: 10.3390/molecules27185953.
19. Pérez-Davila, S.; González-Rodríguez, L.; Lama, R.; López-Álvarez, M.; Oliveira, A.L.; Serra, J.; Novoa, B.; Figueras, A.; González, P. 3D-Printed PLA Medical Devices: Physicochemical Changes and Biological Response after Sterilisation Treatments. *Polymers*. **2022**, 14, 4117. doi: 10.3390/polym14194117
20. Eutionnat-Diffo, P.A.; Chen, Y.; Guan, J.; Cayla, A.; Campagne, C.; Zeng, X.; Nierstrasz, V. Stress, Strain and Deformation of Poly-Lactic Acid Filament Deposited onto Polyethylene Terephthalate Woven Fabric Through 3D Printing Process. *Sci. Rep*. **2019**, 9, 14333. doi: 10.1038/s41598-019-50832-7
21. Spahiu, T.; Canaj, E.; Shehi, E. 3D Printing for Clothing Production. *J. Eng. Fibers Fabr*. **2020**, 15, 1-8. doi: 10.1177/1558925020948216
22. Kalita, N.K.; Damare, N.A.; Hazarika, D.; Bhagabati, P.; Kalamdhad, A.; Katiyar, V. Biodegradation and Characterization Study of Compostable PLA Bioplastic Containing Algae Biomass as Potential Degradation Accelerator. *Environ. Chall*. **2021**, 3, 100067. doi: 10.1016/j.envc.2021.100067
23. Buddhakala, M.; Buddhakala, N. Physical, Mechanical and Antibacterial Properties of Biodegradable Bioplastics from Polylactic Acid and Corncob Fibers with Added Nano Titanium Dioxide. **Trends Sci. 2023**, 20(4), 6473. doi: 10.48048/tis.2023.6473

24. Tsioptsias C.; Tsivintzelis I. On the Thermodynamic Thermal Properties of Quercetin and Similar Pharmaceuticals. *Molecules*. **2022**, 27(19), 6630. doi: 10.3390/molecules27196630
25. Syed Draman, S.F.; Daik, R.; Abdul Latif, F.; El-Sheikh, S.M. Characterization and Thermal Decomposition Kinetics of Kapok (*Ceiba pentandra* L.)–Based Cellulose. *BioResources*. **2013**, 9(1), 8-23.
26. Neto, J.S.S.; de Queiroz, H.F.M.; Aguiar, R.A.A.; Banea, M.D. A Review on the Thermal Characterisation of Natural and Hybrid Fiber Composites. *Polymers.* **2021**, 13, 4425. doi: 10.3390/polym13244425
27. Karvran, M.; Vagner, C.; Cochez, M.; Ponçot, M.; Saeb, M.R.; Vahabi, H. Thermal Degradation of Polylactic Acid (PLA)/Polyhydroxybutyrate (PHB) Blends: A Systematic Review. *Polym. Degrad. Stab*. **2022**, 201, 109995.
28. Du, Q.; Chen, Y.N. R & D Status and Countermeasures of Natural Functional Kapok Fiber. *Adv. Mat. Res*. **2013**, 796, 199-204. doi: 10.4028/www.scientific.net/amr.796.199
29. Hu, L., Wang, F., Xu, G., Xu, B. Unique Microstructure of Kapok Fibers in Longitudinal Microscopic Images. *Text. Res. J*. **2017**, 87(18), 2255-2262. doi: 10.1177/0040517516673334
30. Koschevic, M.T.; Araújo, R.P.; Garcia, V.A.; Fakhouri, F.M.; Oliveira, K.M.P.; Arruda, E.J.; Dufresne, A.; Martelli, S.M. Antimicrobial Activity of Bleached Cattail Fibers (*Typha domingensis*) Impregnated with Silver Nanoparticles and Benzalkonium Chloride. *J. Appl. Polym. Sci.* **2021**, 138(35), 50885. doi: 10.1002/app.50885
31. Mwaikambo, L.Y. Review of the History, Properties and Application of Plant Fibres. *AJST*. **2006**, 7(2), 120-133.
32. Sekar, V.; Fouladi, M.H.; Namasivayam, S.N.; Sivanesan, S. Additive Manufacturing: A Novel Method for Developing an Acoustic Panel Made of Natural Fiber-Reinforced Composites with Enhanced Mechanical and Acoustical Properties. *J. Eng*. **2019**, 4546863. doi: 10.1155/2019/4546863
33. Wu, S.; Zhang, J.; Li, C.; Wang, F.; Shi, L.; Tao, M.; Weng, B.; Yan, B.; Guo, Y.; Chen, Y. Characterization of Potential Cellulose Fiber from Cattail Fiber: A Study on Micro/Nano Structure and Other Properties. *Int. J. Biol. Macromol.* **2021**, 193(A), 27-37. doi: 10.1016/j.ijbiomac.2021.10.088
34. Du, B.; Li, Z.; Bai, H.; Li, Q.; Zheng, C.; Liu, J.; Qiu, F.; Fan, Z.; Hu, H.; Chen, L. Mechanical Property of Long Glass Fiber Reinforced Polypropylene Composite: From Material to Car Seat Frame and Bumper Beam. *Polymers*. **2022**, 14, 1814. doi: 10.3390/polym14091814
35. Lim, T.T.; Huang, X. Evaluation of Hydrophobicity/Oleophilicity of Kapok and Its Performance in Oily Water Filtration: Comparison of Raw and Solvent-Treated Fibers. *Ind. Crops Prod*. **2007**, 26(2), 125-134. doi: 10.1016/j.indcrop.2007.02.007
36. Futalan, C.M.; Choi, A.E.S.; Soriano, H.G.O.; Cabacungan, M.K.B.; Millare, J.C. Modification Strategies of Kapok Fiber Composites and Its Application in the Adsorption of Heavy Metal Ions and Dyes from Aqueous Solutions: A Systematic Review. *Int. J. Environ. Res. Public Health.* **2022**, 19(5), 2703. doi:10.3390/ijerph19052703.
37. Cui, Y.; Xu, G.; Liu, Y. Oil Sorption Mechanism and Capacity of Cattail Fiber Assembly. *J. Ind. Text.* **2014**, 43(3), 330-337. doi:10.1177/1528083712452902
38. Abdullah, M.A.; Rahmah, A.U.; Man, Z. Physicochemical and Sorption Characteristics of Malaysian *Ceiba pentandra* (L.) Gaertn. as a Natural Oil sorbent. *J. Hazard Mater.* 2010, 177(1-3), 683-91. doi: 10.1016/j.jhazmat.2009.12.085
39. Draman, S.F.S.; Daik, R.; Latif, F.A.; El-Sheikh, S.M. Characterization and Thermal Decomposition Kinetics of Kapok (*Ceiba pentandra* L.)–Based Cellulose. *Bioresour.* **2014**, 9(1), 8-23.
40. Wu, S.; Zhang, J.; Li, C.; Wang, F.; Shi, L.; Tao, M.; Weng, B.; Yan, B.; Guo, Y.; Chen, Y. Characterization of Potential Cellulose Fiber from Cattail Fiber: A Study on Micro/Nano Structure and Other Properties. *Int. J. Biol. Macromol.* **2021**, 193, 27-37. doi: 10.1016/j.ijbiomac.2021.10.088
41. Behera, B.K.; Arora, H. Surgical Gown: A Critical Review. *J. Ind. Text.* **2009**, 38(3), 205–231. doi: 10.1177/1528083708091251
42. Baraniak, J.; Kania-Dobrowolska, M. Multi-Purpose Utilization of Kapok Fiber and Properties of *Ceiba Pentandra* Tree in Various Branches of Industry. *J. Nat. Fibers*. **2023**, 20(1), 2192542. doi: 10.1080/15440478.2023.2192542
43. Kannekens, A. Breathable Coatings and Laminates. *J. Coated Fabrics*. **1994**, 24, 51-59.